

# INFLUENCE OF THE GEOMETRICAL PARAMETERS OF URBAN CANYONS ON THE CONVECTIVE HEAT TRANSFER COEFFICIENT

*Andrea VALLATT<sup>a</sup>, Giorgio GALLI<sup>a</sup>, Chiara COLUCCI<sup>a</sup>, Pawel OCLON<sup>b,\*</sup>*

<sup>a</sup> Department of DIAEE, Sapienza University of Rome, Via Eudossiana 18, 00184 Rome, Italy

<sup>b</sup> Institute of Thermal Power Engineering, Cracow University of Technology, al. Jana Pawła II 37, PL-31-864 Kraków, Poland

E-mail: poclon@mech.pk.edu.pl (corresponding author)

*Abstract. In this study, a microclimate analysis has been carried out starting with a particular urban configuration, "the street canyon". The analysis, conducted by performing numerical simulations using the finite volumes commercial code ANSYS-Fluent studies how the thermal and flow field are affected by the effect of the solar radiation, varying the ratio  $H/W$ . Furthermore, a thermo-fluid dynamic analysis of natural convection effects and of 3D characteristics of the flow field on the heat transfer coefficient, has been carried out. The check of the urban microclimate through this type of study, can be helpful to find solutions at thermal comfort and energy saving.*

*Key words: urban canyon; solar radiation; computational fluid dynamics (CFD); urban microclimate.*

## 1. Introduction

The well-being and quality of life of each of us also depend on the climatic conditions environment where we live [1]. Considering that about 50% of the world population live in urban areas [2], it is natural and necessary to study the characteristics of the microclimate of our urban areas. In particular, the climatic conditions and urban environment appear closely related to the morphological characteristics of the city (and the parts of this). In many cases, urbanization can affect the local climate of a city more intensely and faster than the global warming giving rise to the phenomenon of the so-called urban heat island (UHI). This study will concentrate on the analysis of a particular urban configuration: the urban canyon. The geometry of the urban canyon is often described by a single parameter, the canyon aspect ratio ( $H/W$ ), which is defined as the ratio of the building height ( $H$ ) to the width between buildings ( $W$ ). In literature several authors have studied the street canyons, through numerical simulations [3], wind tunnel experiments [4-6], measurement campaigns [7], and comparison between numerical model and measurements campaign on a canyon scale model [8]. In literature, there are typically two-dimensional studies [3, 9]. Three-dimensional effects are considered in other studies [4, 5] but an array of cubical buildings is simulated, and in this case, the flow is channeled and it maybe supposed that the tridimensional effects are less important. In this paper, using a commercial CFD code (Ansys Fluent), an isolated street canyon is considered, to

evaluate how the flow field changes within the canyon at different H/W ratio and to highlight the importance of considering tridimensional effects on convective heat transfer inside the canyon.

In some papers, not only the canyon but also the urban configuration around the canyon, are studied numerically [10, 11]. In [12] the effects of the radiative properties of the surfaces materials on canyon surfaces temperatures and their importance for heat island mitigation are evaluated. In the study of urban microclimate in an urban canyon the convective heat transfer coefficients (CHTC) analysis, for external surfaces of the building, play a key role. The analysis of thermal and the flow fields in an urban canyon provides the surfaces values of parameters like CHTC and friction velocity that are required by UHI models [13, 14].

The thermal field and flow field inside an urban canyon are two basic parameters for the analysis of heat exchanges between confined environment and open space. In this particular study, we analyze, just how they are affected by the ratio H/W while L/H is fixed. The analysis of the flow and thermal field inside of the canyon has been performed with a CFD simulations conducted during summer days, because, during this period, weather conditions affect human activity much more than during the winter season. The thermal field is determined by setting up the solar radiation module, the ambient conditions and thermophysical properties values of the buildings and the ground.

## 2. CFD Numerical Model

The simulations have been performed with the commercial CFD code Ansys Fluent 14.0, 3D double precision, pressure based version and the steady RANS (Reynolds-averaged Navier–Stokes) equations have been solved in combination with the standard k-  $\varepsilon$  model. The governing equations can be expressed as follows.

Momentum equation:

$$\bar{u}_j \frac{\partial \bar{u}_i}{\partial x_j} = -\frac{1}{\rho} \frac{\partial \bar{p}}{\partial x_i} + \frac{\mu}{\rho} \frac{\partial^2 \bar{u}_i}{\partial x_i \partial x_j} - \frac{\partial}{\partial x_j} (\overline{u'_i u'_j}) + f_i \quad (1)$$

Continuity equation:

$$\frac{\partial \bar{u}_i}{\partial x_i} = 0 \quad (2)$$

Heat conservation equation:

$$\bar{u}_i \frac{\partial \bar{T}}{\partial x_i} + \frac{\partial}{\partial x_i} \left( K_T \frac{\partial \bar{T}}{\partial x_i} \right) = 0 \quad (3)$$

where  $\bar{u}_i$  is the average speed of air flow;  $\overline{u'_i u'_j}$  is the Reynolds stress;  $\rho$  is the air density;  $\mu$  is the molecular viscosity;  $f_i$  is the thermal-induced buoyant force;  $\bar{T}$  is the potential temperature;  $K_T$  is the heat diffusivity. The standard k-  $\varepsilon$  model has been used to solve the turbulence problem. The turbulence kinetic energy,  $k$ , and its rate of dissipation,  $\varepsilon$ , are obtained from the following transport equations:

$$\frac{\partial}{\partial t} (\rho k) + \frac{\partial}{\partial x_i} (\rho k u_i) = \frac{\partial}{\partial x_j} \left[ \left( \mu + \frac{\mu_t}{\sigma_k} \right) \frac{\partial k}{\partial x_j} \right] + G_k + G_b - \rho \varepsilon \quad (4)$$

and

$$\frac{\partial}{\partial t} (\rho \varepsilon) + \frac{\partial}{\partial x_i} (\rho \varepsilon u_i) = \frac{\partial}{\partial x_j} \left[ \left( \mu + \frac{\mu_t}{\sigma_\varepsilon} \right) \frac{\partial \varepsilon}{\partial x_j} \right] + C_{1\varepsilon} \frac{\varepsilon}{k} (G_k + C_{3\varepsilon} G_b) - C_{2\varepsilon} \rho \frac{\varepsilon^2}{k} \quad (5)$$

where:

$G_k$  is the generation of turbulence kinetic energy due to the mean velocity gradients;  $G_b$  is the generation of turbulence kinetic energy due to buoyancy;  $C_{1\varepsilon}$ ,  $C_{2\varepsilon}$  and  $C_{3\varepsilon}$  constants and the  $K_T$  and  $\mu_t$  expressions are reported in the standard k-  $\varepsilon$  model of Ansys Fluent 14.0, 2011;  $\sigma_k$  and  $\sigma_\varepsilon$  are the

turbulent Prandtl numbers for  $k$  and  $\varepsilon$ , respectively. To evaluate the impact of thermal effects, the incompressible ideal gas module has been used for air density.

In this model the Standard wall functions (SWFs) are used to save computing time.

The formula used to evaluate the CHTC coefficient is reported following:

$$CHTC = \frac{q}{T_{wall} - T_{ref}} \quad (6)$$

Where:

$q$  is the convective heat flux,  $T_{wall}$  is the wall temperature, and  $T_{ref}$  is the reference temperature defined in the boundary conditions.

In [15] it is shown that in urban canyons the standard wall function (SWF) give CHTC that agree with LRNM (Low-Reynolds Number Modeling), if natural convection effects are moderate and when the Richardson number (Ri) is not much higher than one. In the present paper the Ri is not larger than 3, then the SWF are used. The aim of this paper is to compare the microclimate for different cases using the same models with the same limitations. In particular, different geometrical configuration are analyzed differing the H/W parameter.

## 2.1. Computational domain

To calculate the thermal effects, the natural convection module has been activated by setting an incompressible ideal gas model for air density. The analyzed urban canyon has the following geometrical characteristics: the aspect ratio H/W = 0,5, H/W=1 and H/W=2 (fig. 1), the orientation is N–S, the width and height of the building are 20 m, the street length is 100 m and the street width is 20 m.

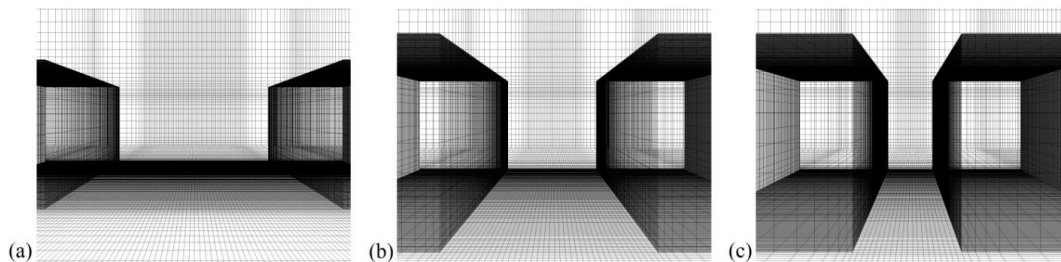


**Figure 1. Canyon with H/W=0.5 (a), H/W=1 (b), H/W=2 (c)**

Based on the best practice guidelines by Franke et al. [16] and Tominaga et al. [17], the dimensions of the computational domain have been chosen in relation to the buildings height  $H$  (fig. 2): the distance between the side walls of the buildings and the north, east and south planes is  $5H = 100$  m, instead the west plane is  $15H = 300$  m from the westerly building. The distance between the roofs of the buildings and the upper plane is  $5H = 100$  m. The building's dimensions determine the different domain extension behind the built area. When the flow direction is transversal to the canyon length, the obstacle size is maximum, and the flow re-development requires a distance of  $15H$  from the buildings to the outflow bounds. Instead, when the flow is parallel to the canyon axis, the obstacle size is minimum, and the distance behind the built area is  $5H$ . The domain dimension over the buildings has been chosen to take into account the blockage ratio, defined as the ratio of the area blocked by the buildings to the total cross-section area. This parameter depends on the obstacles size and wind direction: when the building obstacle area is minimum, the blockage ratio assumes the value of 2%, instead of when the wind impacts transversally to the canyon direction, it assumes the maximum value of 5.5%. To ensure a high quality of the computational grid, it is fully structured, and the shape of the

cells has been chosen hexahedral (fig. 1). To simulate flow fields, in the area of interest, 40 cells per cube root of the building volume has been used and 20 cells per building separation [16]. For the vertical resolution of the canyon 20 cells have been used. Furthermore, the grid has been arranged so that the evaluation height for pedestrian comfort is located higher than the 3rd grid from the ground surface.

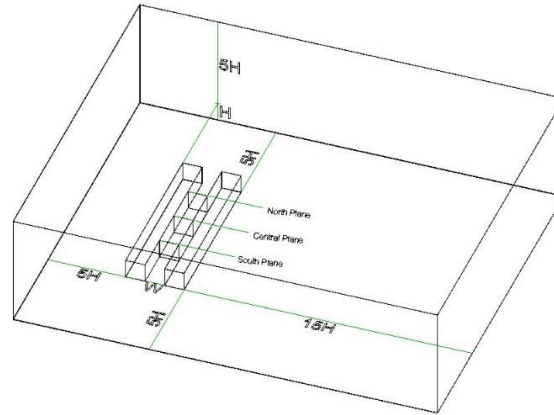


**Figure 2. Computational domain**

## 2.2. Boundary conditions

In this simulation, the surfaces temperatures have been obtained as the result of the heat transfer calculations, setting up: the temperature of the undisturbed air, the solar load module and the temperature inside of the buildings (299 K). To evaluate the soil influence, the calculation domain has been extended 5 m below the ground level. The ground has been simulated with the following thermophysical characteristics: thermal conductivity = 2 W/m·K; temperature at  $-5$  m = 288 K; density = 1000 kg/m<sup>3</sup>; specific heat = 1000 J/kg·K; solar radiation absorptivity (visible and infrared) = 0.8; emissivity = 0.9. The radiation exchanges have been calculated setting up the S2S radiation model, in which the energy exchange parameters are considered by a geometric function, *i.e.*, view factor, and activating the solar ray tracing. The zero static pressure on the outlet plane and zero gradients of all variables at the top and lateral sides of the domain are setting. Transient heat conduction in ground and walls has been analyzed in [18]. This study finds that thermal inertial effects are important to calculate heat fluxes and the temperatures of the inner layers, but not for surface temperatures which influence the natural convection flow fields. In [18] it's shown that the differences between the surfaces temperatures of the steady state and the transient case are a few percent of the air surface temperature difference so that only steady state simulation have been carried out. Furthermore, the materials characteristics have been reported in [16, 17]: the building walls have: thermal conductivity = 0.15 W/(mK); specific heat = 1000 J/(kgK); density = 1000 kg/m<sup>3</sup>; internal air temperature = 299 K; thickness = 0.30 m; emissivity = 0.9. In [18] it has been verified that as the flow approaches the built area the inlet velocity profile is fully-developed before reaching the buildings and it can be represented by Equation (7), where  $u^*$  is the friction velocity,  $K$  is the Von Karman constant (0.4),  $z$  is the height coordinate and  $z_0$  is the aerodynamic roughness and its value is 0.05 m that can be considered an appropriate value to represent the roughness of the land covered with low vegetation and small isolated obstacles [19]. This equation represents the wind velocity profile of the inlet flow when the

wind approaches the buildings. In another study [18], it is shown that the wind profile reaches the asymptotic velocity when it reaches about 4 m in height.

$$u(z) = \frac{u^*}{K} \ln\left(\frac{z+z_0}{z_0}\right) \quad (7)$$

The friction velocity value has been obtained by the correlation with the calculated value of the turbulent kinetic energy ( $k$ ) at the first node above the ground, as shown in Equation (8) [16].

$$u^* = K^{0.5} \cdot C_\mu^{0.25} \quad (8)$$

where  $C_\mu = 0.09$ ; on the buildings facades and the ground inside the canyon the roughness length is zero.

### 2.3. Model validation

The validation of the mathematical model used in our study has been carried out through the comparison with the wind tunnel experiment performed by Uehara [4]. The experiment has been characterized by a flow direction transversal to rows of blocks and, at the measurement location, the flow appeared totally canalized. A numerical validation test has been performed on our street canyon model, which has been scaled by the reduction factor 1/200 and where the wind direction has been considered totally transversal to the canyon direction. The comparison between the data obtained with the wind tunnel experiments and the numerical test has been carried out for the vertical profile of normalized horizontal velocity  $u/u_0$  and  $(T-T_f)/(T_a-T_f)$ , evaluated on a central vertical line within the street canyon. The agreement between the numerical model and the wind tunnel experiments is satisfactory inside the canyon as shown in [18] where the experimental and numerical model results are plotted and they agree well inside the canyon.

### 3. Results

The H/W ratio is a very important value to define airflow and temperature fields inside the canyon. For this reason, six simulations were performed: three at 11:00 a.m. 21st of July with H/W = 0.5, 1, 2 (fig. 1); three at 02:00 p.m. on the 21st of July for the same value of H/W. The canyon is made by two twin buildings with H=20 m (height), W=20 m (width) and L=100 m (length), is North-South oriented, placed in Milan, Italy (Lat = 9.18, Long = 45.47, UTC +1). In each simulation, fixed values of ambient wind velocity magnitude and wind direction and undisturbed air temperature, have been considered ( $u_0 = 2$  m/s, wind direction = 45°N and undisturbed air temperature 303 K). The velocity value of 2 m/s has been chosen because the effect of natural convection is still important [5]. As found in [18, 20, 21], the values of CHTC are not very sensitive to wind direction neither for isolated buildings [21] nor inside canyons [18, 20].

As reported in [21], the values of CHTC on the WW facade in a standalone building, do not show variations in a wide range of wind directions. In particular, in [21] is shown that the CHTC are relatively insensitive to wind direction within the interval 0° +60° from the normal to the WW facade. Important changes are found for wind directions almost parallel to the facade.

Then, in [20] several simulations were performed by varying the wind directions. Particularly for three different wind directions: 20°, 45° and 70° from the canyon axis. As can be seen in tab. 1 [20] the average values of the CHTC on WW and LW facades are similar for three directions. In [18]

instead, have been performed a 2D simulation and a 3D simulation with wind direction perpendicular to the canyon axis. The average value of CHTC on LW and WW are different from the values for other wind directions [20]. Particularly lower values of the CHTC and comparable with the values reported in [22, 23] for 2D canyons are found. Then, the wind direction strongly affects the thermal and dynamical effects within the canyon for wind directions close to the perpendicular to the canyon axis. There is also a large range of wind directions between  $70^\circ$  and  $20^\circ$  from the canyon axis where the influence of the wind direction is low. So that a wind direction of  $45^\circ$  from the canyon axis can represent a wide range of wind directions between  $0^\circ$  and  $60^\circ$ .

To consider the relationship between the wind flow field and temperature field inside the canyon, the values of heat exchange coefficient  $h_c$ , turbulent kinetic energy  $k$ , wall temperatures  $T_{wall}$  and the intensity of the wind speed  $u$  are considered. All variables are calculated on vertical lines on three different planes, with XZ coordinates (fig. 2): the north plane is situated ten meters from the north limit of the building, the central plane is located in the middle of the canyon, and the south plane is ten meters from the south limit. While wall temperatures and heat exchange coefficients are calculated on lines that are situated on the building façades, the turbulent kinetic energy and wind speed are considered on the first node.

Thermal effects considerably modify flow fields inside the canyon. As shown in [20], in which the flow field is analyzed inside an urban canyon similar to the one of this paper, when the natural convection is not considered, a single aerodynamic vortex can be formed in the canyon. When natural convection is switched on two counter-rotating vortices of which one is aerodynamic, and the other one is thermal are often formed in the canyon. These effects are reported in several papers for instance [3].

Results of calculated simulation, always considered with natural convection, are consistent with the cited simulation, as is visible from fig. 3, in which the wind velocity vectors are represented, calculated in South vertical plane with different H/W at 02:00 p.m.

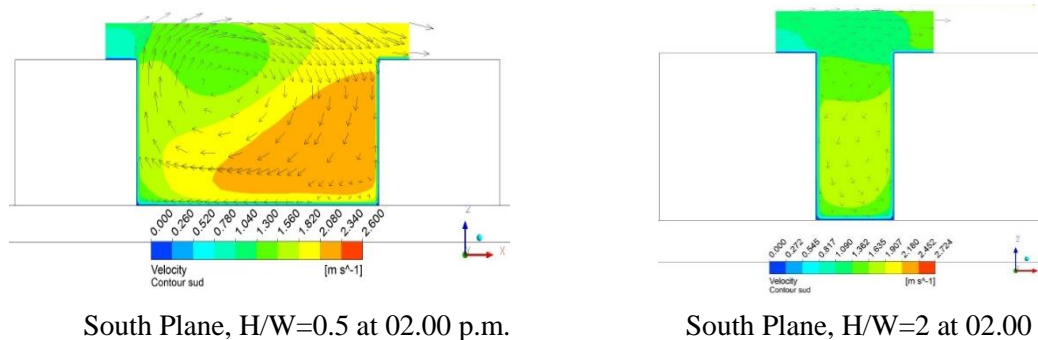


**Figure 3. Wind flow field on XZ south plan with H/W=2 and 0.5**

As can be seen from fig. 3, in South Plane with H/W=0.5 we only have one vortex while in South Plane with H/W=2 is evident in the bottom WW façade the presence of a second vortex due to convective aspects.

### 3.1. Average values of CHTC inside of the canyon

Table 1, shows surface averaged values of  $h_c$  in the windward and leeward façade for the three values of H/W ratio and the values for the same configurations for the 2D studies implemented by [22, 23]. In particular, the results relevant to a numerical computation performed for a 2D canyon, with

natural convection switched on, using a wall temperature of 30°C and an incoming air temperature of 20°C [23], are displayed in tab. 1

**Table 1. Values of the  $h_c$  parameter on the windward at 02:00 pm and Leeward façade at 11:00 am in present study and on others studies present in literature.**

	H/W = 0.5		H/W = 1			H/W = 2	
	[23]	Present Study	[23]	[22]	Present Study	[23]	Present Study
WW	3.55	11.57	3.16	3.08	11.28	2.03	9.91
LW	2.41	10.51	2.38	2.22	10.29	1.83	9.28

. A result obtained by Saneinejad [22] using a 2D configuration with  $H/W = 1$ , the natural convection switched off, wind velocity 2 m/s, incoming air temperature 20°C and wall uniform temperatures 30°C is also reported. As regards the values of  $h_c$  in relation to the  $H/W$  from tab. 1 is seen that there is a slight decrease with the increase of  $H/W$  which becomes more evident between  $H/W = 1$  and 2.

The average values of CHTC on the leeward façade are always lower than those of the windward façade coherently with the other papers in the literature, but in our case, the difference is lower. The same trend was found by Allegrini et al. [23] with a much higher decrease of  $h_c$ . In our case, we arrive at 10% in Allegrini's case also to 30%. The results of Allegrini [23] and Saneinejad [22] show much lower values of CHTC than those obtained in this study and this appears to be because considered a bidimensional case.

As it can be seen in [18, 20, 22, 23, 24], the flow field inside the urban canyon in the 2D simulations is different from the flow corresponding to 3D simulations for wind directions not normal to the canyon axis. In particular, in the 2D case, the flow field is characterized by a skimming flow and, for the same external air velocity, the values of the wind velocity inside the urban canyon are lowered than in the 3D case. Of course, the values of the CHTC are lower.

### 3.2. Tridimensional effects inside the canyon

Table 2 and Table 3 shows values of dynamic and thermal variables relatively to the windward and leeward façade at 11:00 a.m. and 02:00 p.m. for the three values of  $H/W$  ratio.

The results reported in tab. 2 and tab. 3 are obtained by simulations in a 3D domain (fig. 2), and three-dimensional effects on the flow are evident in the formation of a spiral flow, made by the combination of a vertical descendent vortex and the longitudinal component of wind speed, as was demonstrated in various studies [5, 20].

The presence of the longitudinal velocity component has an important effect on the characteristics of the flow field, and determines much greater values of CHTC than those typical of the two-dimensional field, as shown in tab. 1. Notice that such a longitudinal component plays a fundamental role also when the wind is almost transversal to the canyon [20].

This longitudinal velocity component significantly changes the vortex structure and the flow field along the entire length of the canyon respect to 2D analysis [18, 20, 21].

Tables 2 and 3 show that the CHTC and turbulent kinetic energy and local velocity values may have considerable variation along the canyon axis.

**Table 2. Values of the parameters on the windward façade at 11:00 a.m. and at 02:00 p.m.**

WINDWARD FAÇADE AT 11:00 A.M.						
RATIO	PLANE	$h_c$ (W/m <sup>2</sup> K)	$k$ (m <sup>2</sup> /s <sup>2</sup> )	$T_{wall}$ (K)	$u$ (m/s)	$u_z$ (m/s)
H/W = 0.5	North	12,48	0,28	307,71	1,44	0,19
	Central	10,34	0,19	308,53	1,52	-0,04
	South	9,81	0,15	308,55	1,69	-0,40
H/W = 1	North	13,79	0,33	308,20	1,82	0,14
	Central	10,03	0,16	309,32	1,61	-0,46
	South	9,02	0,12	310,27	1,39	-0,47
H/W = 2	North	13,32	0,30	307,99	1,88	0,11
	Central	8,77	0,11	310,19	1,38	-0,36
	South	7,41	0,08	312,09	1,18	-0,26
WINDWARD FAÇADE AT 02:00 p.m.						
RATIO	PLANE	$h_c$ (W/m <sup>2</sup> K)	$k$ (m <sup>2</sup> /s <sup>2</sup> )	$T_{wall}$ (K)	$u$ (m/s)	$u_z$ (m/s)
H/W = 0.5	North	12,50	0,28	323,55	1,44	0,23
	Central	11,04	0,23	325,69	1,49	0,16
	South	11,19	0,22	325,37	1,63	-0,08
H/W = 1	North	13,72	0,33	321,19	1,81	0,20
	Central	10,56	0,19	324,67	1,52	-0,20
	South	9,57	0,14	326,64	1,41	-0,09
H/W = 2	North	13,18	0,30	319,44	1,87	0,16
	Central	9,06	0,12	324,51	1,33	-0,11
	South	7,50	0,09	327,85	1,22	0,29

These variations of CHTC and  $k$  can be connected with the three-dimensional nature of the flow field as seen from fig.4. In de Lieto Vollaro A. et al. [24] and by fig. 4, it can be seen that at the North plane the flow field structure is the same for each H/ W parameter and different from that on the other planes. In particular, the direction of the flow field in North plane is characterized by the external velocity field, and the velocity vectors have the predominant component perpendicular to WW façade. This creates a strong recirculation and thus a turbulent kinetic energy increase. Moreover, as can be seen from tab. 2, 3 the turbulent kinetic energy is strongly correlated with the values of CHTC: it can be seen that CHTC coefficient and  $K$  vary in similar ways, while CHTC and the local velocity value on the wall may vary in opposite ways, in particular in LW façade. Also in [21] it is shown that on the WW façade of an isolated building the local values of the CHTC are better correlated with  $K$  than with the local velocities.

From Central plane to the South plane, the aerodynamic vortex coming from the roof is fully-developed (figs. 3 and 4). In particular, it is seen that for H/W = 0.5 the second natural convection vortex which rotates in the opposite direction is not evident, but the CHTC and the turbulent kinetic



energy are higher when the wall is radiated by the sun. Instead for  $H/W=1$  the second vortex due to convective aspects on the central plane appears in bottom WW facade. For  $H/W = 2$  on the central and south planes the second vortex occupies a large part of the canyon. It is, therefore, clear the importance of natural convection in the formation of the opposite vortex. From tabs. 2 and 3 it can be seen that variations of the CHTC values there are along the canyon axis and this variations also depend on the  $H/W$  parameter.

**Table 3. Values of the parameters on the leeward façade at 11:00 a.m. and at 02:00 p.m.**

LEEWARD FAÇADE AT 11:00 A.M.						
RATIO	PLANE	$h_c$ (W/m <sup>2</sup> K)	$k$ (m <sup>2</sup> /s <sup>2</sup> )	$T_{wall}$ (K)	$u$ (m/s)	$u_z$ (m/s)
H/W = 0.5	North	10,16	0,22	325,64	1,11	0,75
	Central	11,16	0,19	324,27	0,77	0,28
	South	10,21	0,18	325,71	1,44	0,72
H/W = 1	North	10,40	0,21	324,38	1,11	0,59
	Central	10,78	0,20	323,90	0,59	0,20
	South	9,69	0,15	325,82	1,50	0,69
H/W = 2	North	11,38	0,24	320,65	1,07	0,34
	Central	8,64	0,13	324,10	0,27	0,09
	South	7,82	0,10	326,39	1,27	0,43
LEEWARD FAÇADE AT 02:00 p.m.						
RATIO	PLANE	$h_c$ (W/m <sup>2</sup> K)	$k$ (m <sup>2</sup> /s <sup>2</sup> )	$T_{wall}$ (K)	$u$ (m/s)	$u_z$ (m/s)
H/W = 0.5	North	8,77	0,13	309,59	0,91	0,58
	Central	9,99	0,17	309,50	0,69	0,22
	South	9,15	0,14	309,95	1,27	0,50
H/W = 1	North	8,76	0,13	309,37	0,52	0,05
	Central	9,44	0,16	310,00	0,88	0,32
	South	8,53	0,12	310,87	1,29	0,33
H/W = 2	North	10,87	0,21	308,26	0,30	-0,01
	Central	7,85	0,10	310,88	1,05	0,10
	South	6,78	0,07	312,63	1,23	0,00

In particular, the CHTC values on WW facade decrease along the canyon axis and this decrease is more accentuated varying  $H/W$ . For  $H/W = 0.5$  and 1 the CHTC variations along the canyon are about of 30%, while for  $H/W = 2$  the variations are about 50%. Instead, on LW façade, those changes are much less marked for  $H/W = 1$  and 0.5 and are considerable only for  $H/W = 2$  (tab. 3).

The results, therefore, seem that there is a strong correlation between the local values of the CHTC and  $H/W$  parameter. In the LW façade for  $H/W=2$  the variations for CHTC is near 40% instead in the WW façade for  $H/W =2$  the variations get to 50% form South plane to North plane.

The values of  $T_{wall}$  depend on various variables: primarily the amount of building surface under irradiation, the wind speed intensity  $u$ , turbulences of the flow field in the proximity of the building façades described by  $k$ , and the thermal exchange coefficient  $h_c$  between the façade and air inside the canyon. The 3D effects of the flow field appear important for the  $T_{wall}$  values. As shown in tab. 2  $T_{wall}$  increases when  $H/W$  increase and can have strong variations along the canyon axis: usually,  $T_{wall}$  of the North plane is lower than at the other two planes and, in some cases, it differs consistently.

Contemporarily there is also a reduction of thermal exchange coefficient, and this determines a reduction of the capacity for the façades to exchange heat and to lower their surface temperature. In tab. 2 at 02.00 p.m.,  $H/W = 2$ , North plane and south plane surface temperatures differ for more than 8 K. This difference is probably due to the strong variations of kinetic energy that determines the effectiveness of the thermal exchanges.

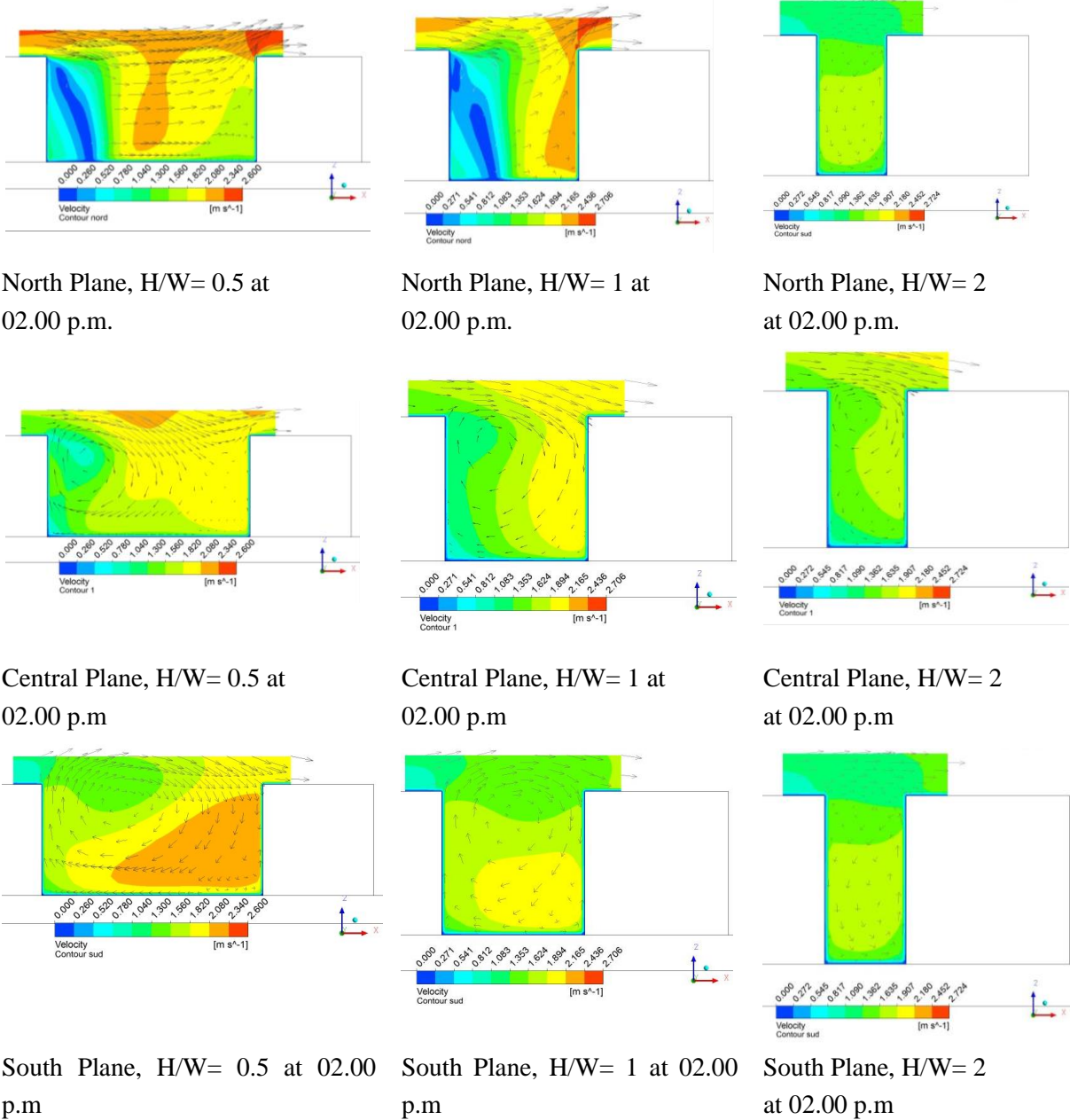


**Figure 4. Wind flow field on XZ north, central and south plan with  $H/W=0.5, 1$  and  $2$ .**

The dependence of various variables on height ( $z$ ) was also analyzed. For the CHTC,  $u$  and  $K$  parameters the dependence of  $z$  (m) exists with increasing  $z$  but is little remarkable, while for  $T_{wall}$  the variations seem important. Figures 5 and 6 report the  $T_{wall}$  parameter on WW and LW façade on the central plane at 11.00 am and 2.00 pm. Figures 5 and 6 show that for both the WW and LW façade, the  $T_{wall}$  in the bottom part of the canyon are higher than the average temperature so that in the

pedestrian part of the canyon the mean radiant temperature is higher and this has a negative effect on the human thermal comfort.

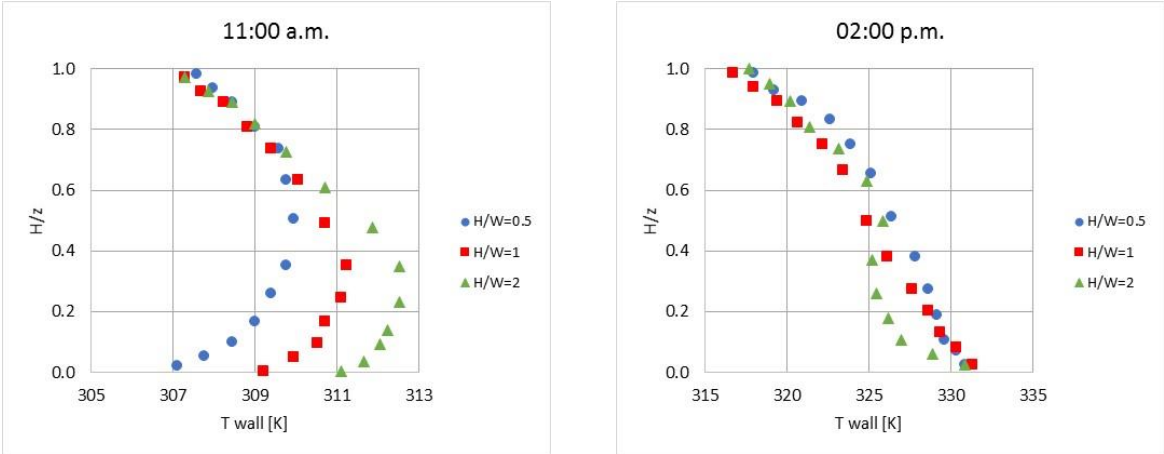


**Figure 5. Trends of  $T_{wall}$  parameter calculated on the windward façade on the central plane within the canyon at 11:00 a.m. and at 02:00 p.m.**

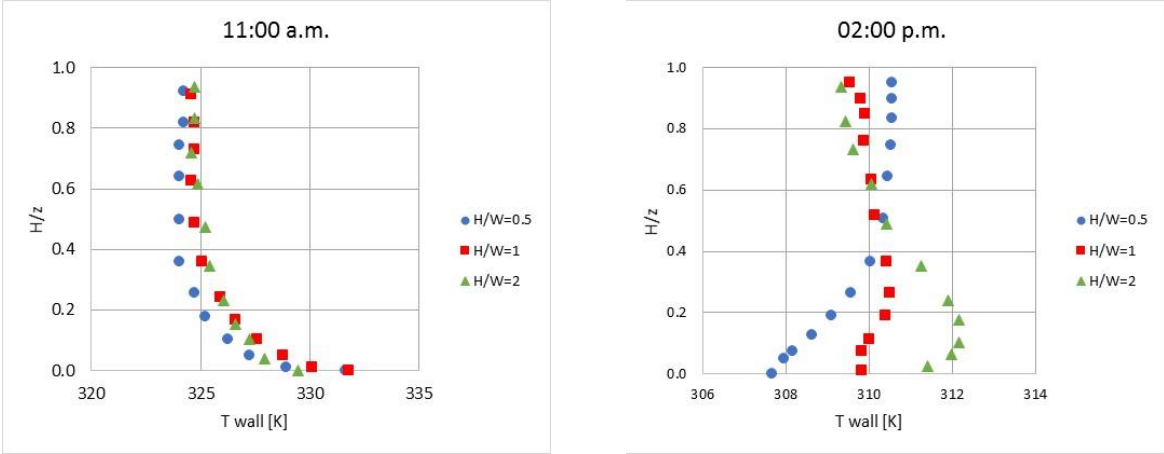


**Figure 6. Trends of  $T_{wall}$  parameter calculated on the leeward façade on the central plane within the canyon at 11:00 a.m. and at 02:00 p.m.**

**Conclusions**

In this numerical study, many different configurations of a 3D urban canyon have been considered by varying the geometric ratio  $H/W$  for two different hours of the day, with the aim to analyze the variations of the thermo-fluid dynamic parameters, *i.e.*  $h_c$ ,  $k$ ,  $T_{wall}$ ,  $u$ , by varying the geometry of the canyon.

The simulations and analysis presented in this paper show that the CHTC coefficient depend on various parameters linked together in a complex way: on the geometric characteristics of the canyon, on incoming solar radiation that influence the natural convection phenomena and on the urban canyon tridimensional characteristic that cause variations on the thermal exchange along the canyon axis

The analysis show that remarkable variations on the thermal exchange and on the CHTC coefficient are found along the canyon axis, for different solar irradiation and geometrical characteristic ( $H/W$ ).

Particularly, in the WW and LW facades the CHTC values for H/W=2 strongly decrease between the inlet and the outlet of the canyon, in the WW façade this variations is about 50% in the LW façade the variations is about 40% maximum. In general it can be said that, the variations of CHTC coefficient along the canyon axis increase with the H/W ratio.

The analysis show that the  $T_{wall}$  parameter increase when H/W increase and can have strong variations along the canyon axis. This phenomenon is directly connected to the natural convection effects and then to the CHTC coefficient. It is evident in the LW façade while it is less noticeable on WW façade where the forced convection effects are more relevant.

These variations on the CHTC coefficients along the canyon axis should be take in to account to evaluate the thermal loads in the buildings on the canyon.

## References

- [1] Moonen, P., *et al.*, Urban physics effect of the micro-climate on comfort, health and energy demand, *Frontiers of Architectural Research*, 1 (2012), pp. 197–228
- [2] United Nations, Department of Economic and Social Affairs, Population Division (2014), *World Urbanization Prospects: The 2014 Revision*, Highlights (ST/ESA/SER.A/352)
- [3] Li, L., *et al.*, Numerical study on the impact of ground heating and ambient wind speed on flow fields in street canyons, *Advances in Atmospheric Sciences*, 29 (2012), pp. 1227–1237
- [4] Uehara, K., *et al.*, Wind tunnel experiments on how thermal stratification affects how in and above urban street canyons, *Atmospheric Environment*, 34 (2000), pp. 1553–1562
- [5] Assimakopoulos, V.D., *et al.*, Experimental validation of a computational fluid dynamics code to predict the wind speed in street canyons for passive cooling purposes, *Solar Energy*, 80 (2006), pp. 423–434
- [6] Tominaga, Y., *et al.*, Wind tunnel analysis of flow and dispersion in cross-ventilated isolated buildings: Impact of opening positions, *Journal of Wind Engineering and Industrial Aerodynamics*, 155 (2016), pp. 74-88
- [7] Offerle, B., *et al.*, Surface heating in relation to air temperature, wind and turbulence in an urban street canyon. *Boundary-Layer Meteorology*, 122 (2007), pp. 273–292
- [8] Blocken, B., *et al.*, Pedestrian-level wind conditions around buildings: Review of wind-tunnel and CFD techniques and their accuracy for wind comfort assessment, *Building and Environment*, 100 (2016), pp. 50-81
- [9] Allegrini, J., *et al.*, Wind tunnel measurements of buoyant flows in street canyons, *Building and Environment*, 59 (2013), pp. 315–326
- [10] Galli, G., *et al.*, Passive cooling design options to improve thermal comfort in an Urban District of Rome, under hot summer conditions, *International Journal of Engineering and Technology*, 5 (2013), 5, pp. 4495–4500
- [11] De Lieto Vollaro, R., *et al.*, Different methods to estimate the mean radiant temperature in an urban canyon, *Advanced Materials Research*, 650 (2013), pp. 647–651

- [12] De Lieto Vollaro, A., *et al.*, Analysis of thermal field within an urban canyon with variable thermophysical characteristics of the building's walls, *Journal of Physics: Conference Series*, 655 (1): 012056, (2015)
- [13] Oleson, K.W., *et al.*, An urban parameterization for a global climate model. Part I: Formulation and evaluation for two cities, *Journal of Applied Meteorology and Climatology*, 47 (2008), pp. 1038–1060
- [14] Masson, V., A physically-based scheme for the urban energy budget in atmospheric models, *Boundary-Layer Meteorology*, 94 (2000), pp. 357–397
- [15] Allegrini, J., *et al.*, An adaptive temperature wall function for mixed convective flows at exterior surfaces of buildings in street canyons, *Building and Environment*, 49 (2012), pp. 55–66
- [16] Franke, J., *et al.*, Best Practice Guideline for the CFD Simulation of Flows in the Urban Environment; COST Action 732, (2007), COST Office: Brussels, Belgium
- [17] Tominaga, Y., *et al.*, AIJ guidelines for practical applications of CFD to pedestrian wind environment around buildings, *Journal of Wind Engineering and Industrial Aerodynamics*, 96 (2008), pp. 1749–1761
- [18] Bottillo, S., *et al.*, Fluid dynamic and heat transfer parameters in an urban canyon, *Solar Energy*, 99 (2013), pp. 1–10
- [19] Montazeri, H., *et al.*, CFD analysis of forced convective heat transfer coefficients at windward building facades: influence of building geometry, *Journal of Wind Engineering and Industrial Aerodynamics*, 146 (2015), pp. 102–116
- [20] Bottillo, S., *et al.*, CFD modeling of the impact of solar radiation in a tridimensional urban canyon at different wind conditions, *Solar Energy*, 102 (2014), pp. 212–222
- [21] Blocken, B., *et al.*, High-resolution CFD simulations for forced convective heat transfer coefficients at the façade of a low rise building, *Building and Environment*, 44 (2009), pp. 2396–2412
- [22] Saneinejad, S., *et al.*, Analysis of convective heat and mass transfer at the vertical walls of a street canyon, *Journal of Wind Engineering and Industrial Aerodynamics*, 99 (2011), pp. 424–433
- [23] Allegrini, J., *et al.*, Analysis of convective heat transfer at building façades in street canyons and its influence on the predictions of space cooling demand in buildings, *Journal of Wind Engineering and Industrial Aerodynamics*, 104 (2012), pp. 464–473
- [24] De Lieto Vollaro, A., *et al.*, Numerical study of urban canyon microclimate related to geometrical parameters, *Sustainability*, 6 (2014), pp. 7894–7905
- [25] Santamouris, M., *et al.*, Thermal and air flow characteristics in a deep pedestrian canyon under hot weather conditions, *Atmospheric Environment*, 33 (1999), pp. 4503–4521

Submitted: 11.05.2017.

Revised: 3.12.2017.

Accepted: 6.12.2017.